

Conformational States of Melittin at a Bilayer Interface

Magnus Andersson,[†] Jakob P. Ulmschneider,[‡] Martin B. Ulmschneider,^{†§} and Stephen H. White^{†*}

[†]Department of Physiology and Biophysics, University of California, Irvine; [‡]Institute of Natural Sciences, Shanghai Jiao Tong University-Shanghai, Shanghai, China; and [§]Department of Crystallography, Institute of Structural and Molecular Biology, University of London, London, United Kingdom

ABSTRACT The distribution of peptide conformations in the membrane interface is central to partitioning energetics. Molecular-dynamics simulations enable characterization of in-membrane structural dynamics. Here, we describe melittin partitioning into dioleoylphosphatidylcholine lipids using CHARMM and OPLS force fields. Although the OPLS simulation failed to reproduce experimental results, the CHARMM simulation reported was consistent with experiments. The CHARMM simulation showed melittin to be represented by a narrow distribution of folding states in the membrane interface.

Received for publication 24 November 2012 and in final form 8 February 2013.

*Correspondence: stephen.white@uci.edu

Magnus Andersson's present address is Science for Life Laboratory, Department of Biochemistry and Biophysics, Stockholm University, SE-106 91 Stockholm, Sweden.

Unstructured peptides fold into the membrane interface because partitioned hydrogen-bonded peptide bonds are energetically favorable compared to free peptide bonds (1–3). This folding process is central to the mechanisms of antimicrobial and cell-penetrating peptides, as well as to lipid interactions and stabilities of larger membrane proteins (4). The energetics of peptide partitioning into membrane interfaces can be described by a thermodynamic cycle (Fig. 1). State A is a theoretical state representing the fully unfolded peptide in water, B is the unfolded peptide in the membrane interface, C is the peptide in water, and D is the folded peptide in the membrane. The population of peptides in solution (State C) is best described as an ensemble of folded and unfolded conformations, whereas the population of peptides in State D generally is assumed to have a single, well-defined helicity, as shown in Fig. 1 A (5). Given that, in principle, folding in solution and in the membrane interface should follow the same basic rules, peptides in state D could reasonably be assumed to also be an ensemble. A fundamental question (5) is therefore whether peptides in state D can be correctly described as having a single helicity. Because differentiating an ensemble of conformations and a single conformation may be an impossible experimental task (5), molecular-dynamics (MD) simulations provide a unique high-resolution view of the phenomenon.

Melittin is a 26-residue, amphipathic peptide that partitions strongly into membrane interfaces and therefore has become a model system for describing folding energetics (3,6–8). Here, we describe the structural dynamics of melittin in a dioleoylphosphatidylcholine (DOPC) bilayer by means of two extensive MD simulations using two different force fields.

We extended a 12-ns equilibrated melittin-DOPC system (9) by 17 μ s using the Anton specialized hardware (10) with the CHARMM22/36 protein/lipid force field and CMAP

correction (11,12) (see Fig. S1 and Fig. S2 in the Supporting Material). To explore force-field effects, a similar system was simulated for 2 μ s using the OPLS force field (13) (see Methods in the Supporting Material). In agreement with x-ray diffraction measurements on melittin in DOPC multilayers (14), melittin partitioned spontaneously into the lipid headgroups at a position below the phosphate groups at similar depth as glycerol/carbonyl groups (Fig. 2).

To describe the secondary structure for each residue, we defined helicity by backbone dihedral angles (ϕ , ψ) within 30° from the ideal α -helical values (-57° , -47°). The per-residue helicity in the CHARMM simulation displays excellent agreement with amide exchange rates from NMR measurements that show a proline residue to separate two helical segments, which are unfolded below Ala⁵ and above Arg²² (15) (Fig. 3 A). In contrast, the OPLS simulation failed to reproduce the per-residue helicity except for a short central segment (see Fig. S3).

Circular dichroism experiments typically report an average helicity of ~70% for melittin at membrane interfaces (3,6,16,17), but other methods yield average helicities as high as 85% (15,18). Our CHARMM simulations are generally consistent with the experimental results, especially amide-exchange measurements (15); melittin helicity averaged to 78% for MLT1, whereas MLT2 transitioned from 75% to 89% helicity at $t \approx 8 \mu$ s, with an overall average helicity of 82% (Fig. 3 B). However, in the OPLS simulation, melittin steadily unfolds over the first 1.3 μ s, after which the peptide remains only partly folded, with an average helicity of 33% (see Fig. S3). Similar

Editor: Scott Feller.

© 2013 by the Biophysical Society

<http://dx.doi.org/10.1016/j.bpj.2013.02.006>



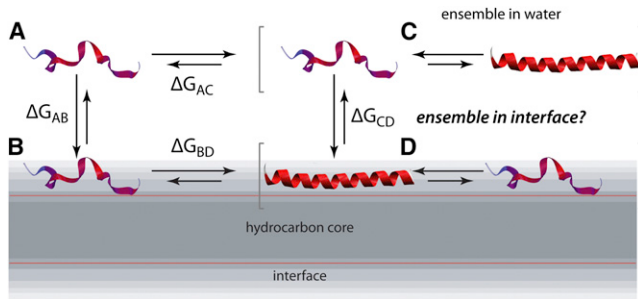


FIGURE 1 Thermodynamic cycles for peptide partitioning into a membrane interface. States A and B correspond to the fully unfolded peptide in solution and membrane interface, respectively. The folded peptide in solution is best described as an ensemble of unfolded and folded conformations (State C). State D is generally assumed to be one of peptides with a narrow range of conformations, but the state could actually be an ensemble of states as in the case of State C.

force-field-related differences in peptide helicity were recently reported, albeit at shorter timescales (19). Although suitable NMR data are not presently available, we have computed NMR quadrupolar splittings for future reference (see Fig. S4).

To answer the question asked in this article—whether the conformational space of folded melittin in the membrane interface can be described by a narrow distribution—the helicity distributions for the equilibrated trajectories are shown in Fig. 3 C. Whereas MLT1 in the CHARMM simulation produces a single, narrow distribution of the helicity, MLT2 has a bimodal distribution as a consequence of the folding event at $t \approx 8 \mu\text{s}$ (Fig. 3 C). We note that CHARMM force fields have a propensity for helix-formation and this transition might therefore be an artifact. We performed a cluster analysis to describe the structure of the peptide in the membrane interface. The four most populated conformations in the CHARMM simulation are shown in Fig. 4.

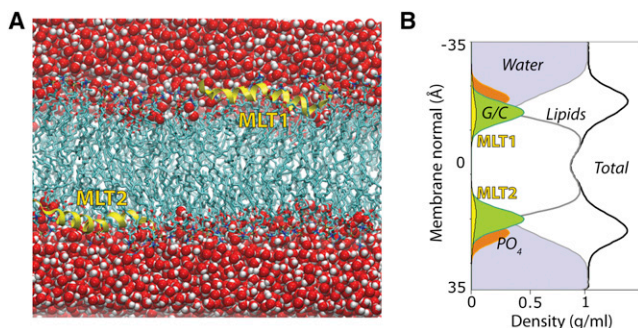


FIGURE 2 Melittin partitioned into the polar headgroup region of the lipid bilayer. (A) Snapshot of the simulation cell showing two melittin molecules (MLT1 and MLT2, in yellow) at the lipid-water interface. (B) Density cross-section of the simulation cell extracted from the 17- μs simulation. The peptides are typically located below the lipid phosphate (PO_4) groups, in a similar depth as the glycerol/carbonyl (G/C) groups.

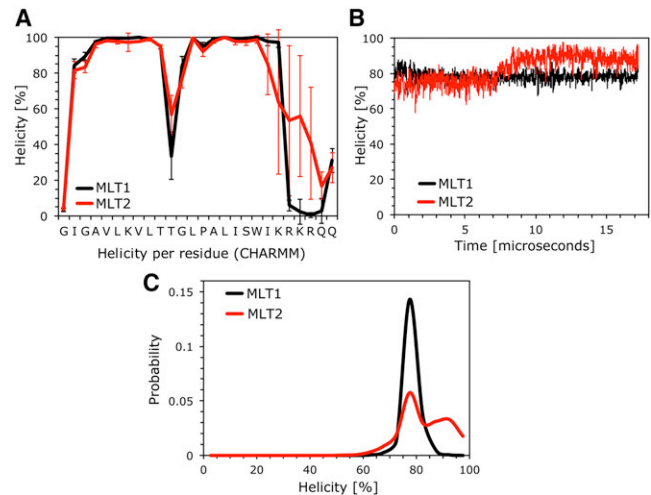


FIGURE 3 Helicity and conformational distribution of melittin as determined via MD simulation. (A) Helicity per residue for MLT1 and MLT2. (B) Corresponding evolution of the helicity. (C) Conformational distributions over the entire 17- μs simulation.

The dominant conformation for both peptides was a helix kinked at G12 and unfolded at the last 5–6 residues of the C-terminus. The folding transition of MLT2 into a complete helix is visible by the 48% occupancy of a fully folded helix.

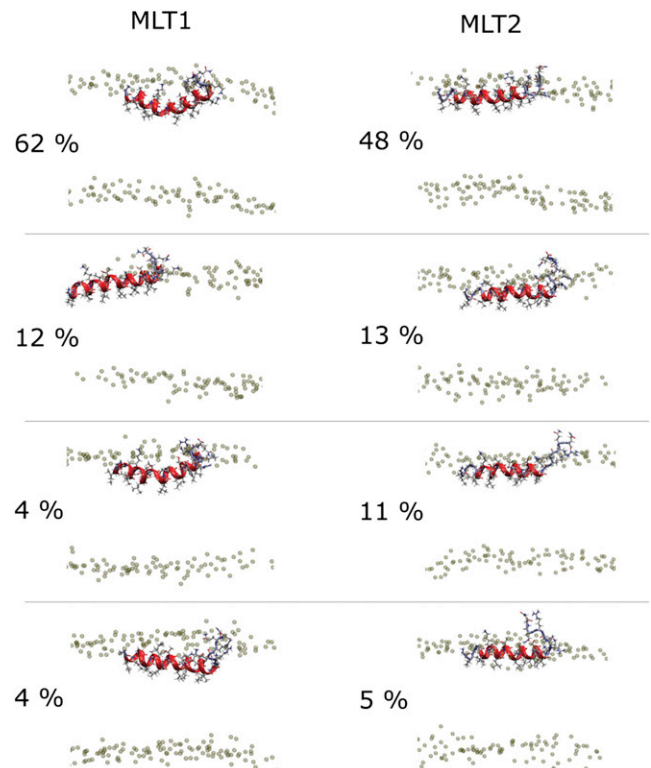


FIGURE 4 Conformational clusters of the two melittin peptides (MLT1 and MLT2) from the 17- μs CHARMM simulation in DOPC. Clustering is based on $\text{C}\alpha$ -RMSD with a cutoff criterion of 2 \AA .

We conclude that the general assumption when calculating folding energetics holds: Folded melittin partitioned into membrane interfaces can be described by a narrow distribution of conformations. Furthermore, extended (several microsecond) simulations are needed to differentiate force-field effects. Although the CHARMM and OPLS simulations would seem to agree for the first few hundred nanoseconds, the structural conclusions differ drastically with longer trajectories, with CHARMM parameters being more consistent with experiments. However, as implied by the difference in substate distributions between MLT1 and MLT2, 17 μ s might not be sufficient to observe the fully equilibrated partitioning process. The abrupt change in MLT2 might indicate that the helicity will increase to greater than experimentally observed in a sufficiently long simulation. On the other hand, it could be nothing more than a transient fluctuation. Increased sampling will provide further indicators of convergence of the helix partitioning process.

SUPPORTING MATERIAL

Four figures, methods, and references (20–27) are available at [http://www.biophysj.org/biophysj/supplemental/S0006-3495\(13\)00191-4](http://www.biophysj.org/biophysj/supplemental/S0006-3495(13)00191-4).

ACKNOWLEDGEMENTS

This work was supported by National Institutes of Health grant No. GM74737 (to S.H.W.) and Program Project No. GM86685 from the National Institute of Neurological Disorders and Stroke, and the National Institute of General Medical Sciences (to S.H.W.) and a Marie Curie International Fellowship (to M.B.U.). M.A. was supported in part by a Senior Postdoctoral Fellowship from the Branches Cost-Sharing Fund through the Institute of Complex Adaptive Matter ICAM, which was itself supported in part by the National Science Foundation. The computations were carried out on the Anton computer at the National Resource for Biomedical Supercomputing at the Pittsburgh Supercomputing Center, which is funded by National Institutes of Health grant No. RC2GM093307.

REFERENCES and FOOTNOTES

- Wimley, W. C., and S. H. White. 1996. Experimentally determined hydrophobicity scale for proteins at membrane interfaces. *Nat. Struct. Biol.* 3:842–848.
- Wimley, W. C., K. Hristova, ..., S. H. White. 1998. Folding of β -sheet membrane proteins: a hydrophobic hexapeptide model. *J. Mol. Biol.* 277:1091–1110.
- Ladokhin, A. S., and S. H. White. 1999. Folding of amphipathic α -helices on membranes: energetics of helix formation by melittin. *J. Mol. Biol.* 285:1363–1369.
- Jayasinghe, S., K. Hristova, and S. H. White. 2001. Energetics, stability, and prediction of transmembrane helices. *J. Mol. Biol.* 312:927–934.
- Almeida, P. F., A. S. Ladokhin, and S. H. White. 2012. Hydrogen-bond energetics drive helix formation in membrane interfaces. *Biochim. Biophys. Acta.* 1818:178–182.
- Vogel, H. 1981. Incorporation of melittin into phosphatidylcholine bilayers. Study of binding and conformational changes. *FEBS Lett.* 134:37–42.
- Kuchinka, E., and J. Seelig. 1989. Interaction of melittin with phosphatidylcholine membranes. Binding isotherm and lipid head-group conformation. *Biochemistry.* 28:4216–4221.
- Beschiaschvili, G., and H.-D. Baeuerle. 1991. Effective charge of melittin upon interaction with POPC vesicles. *Biochim. Biophys. Acta.* 1068:195–200.
- Benz, R. W., H. Nanda, ..., D. J. Tobias. 2006. Diffraction-based density restraints for membrane and membrane-peptide molecular dynamics simulations. *Biophys. J.* 91:3617–3629.
- Shaw, D. E., M. M. Deneroff, ..., S. C. Wang. 2007. Anton, a special-purpose machine for molecular dynamics simulation. Proceedings of the 34th Annual International Symposium for the Computer Architect. *Comm. ACM.* 51:91–97.
- MacKerell, Jr., A. D., M. Feig, and C. L. Brooks, 3rd. 2004. Extending the treatment of backbone energetics in protein force fields: limitations of gas-phase quantum mechanics in reproducing protein conformational distributions in molecular dynamics simulations. *J. Comput. Chem.* 25:1400–1415.
- Klauda, J. B., R. M. Venable, ..., R. W. Pastor. 2010. Update of the CHARMM all-atom additive force field for lipids: validation on six lipid types. *J. Phys. Chem. B.* 114:7830–7843.
- Jorgensen, W. L., D. S. Maxwell, and J. Tirado-Rives. 1996. Development and testing of the OPLS all-atom forcefield on conformational energetics and properties of organic liquids. *J. Am. Chem. Soc.* 118:11225–11236.
- Hristova, K., C. E. Dempsey, and S. H. White. 2001. Structure, location, and lipid perturbations of melittin at the membrane interface. *Biophys. J.* 80:801–811.
- Dempsey, C. E., and G. S. Butler. 1992. Helical structure and orientation of melittin in dispersed phospholipid membranes from amide exchange analysis in situ. *Biochemistry.* 31:11973–11977.
- Almeida, P. F., and A. Pokorny. 2009. Mechanisms of antimicrobial, cytolytic, and cell-penetrating peptides: from kinetics to thermodynamics. *Biochemistry.* 48:8083–8093.
- Ladokhin, A. S., M. Fernández-Vidal, and S. H. White. 2010. CD spectroscopy of peptides and proteins bound to large unilamellar vesicles. *J. Membr. Biol.* 236:247–253.
- Vogel, H., and F. Jähnig. 1986. The structure of melittin in membranes. *Biophys. J.* 50:573–582.
- Ulmschneider, J. P., J. C. Smith, ..., E. Strandberg. 2012. Reorientation and dimerization of the membrane-bound antimicrobial peptide PGLa from microsecond all-atom MD simulations. *Biophys. J.* 103:472–482.
- Shan, Y., J. L. Klepeis, ..., D. E. Shaw. 2005. Gaussian split Ewald: a fast Ewald mesh method for molecular simulation. *J. Chem. Phys.* 122:054101–054113.
- Humphrey, W., A. Dalke, and K. Schulten. 1996. VMD: visual molecular dynamics. *J. Mol. Graph.* 14:33–38.
- Berendsen, H. J. C., D. van der Spoel, and R. van Drunen. 1995. GRO-MACS: a new message-passing parallel molecular dynamics implementation. *Comput. Phys. Commun.* 91:43–56.
- Jorgensen, W. L., J. Chandrasekhar, ..., M. L. Klein. 1983. Comparison of simple potential functions for simulating liquid water. *J. Chem. Phys.* 79:926–935.
- Ulmschneider, J. P., and M. B. Ulmschneider. 2009. United atom lipid parameters for combination with the optimized potentials for liquid simulations all-atom force fields. *J. Chem. Theory Comput.* 5:1803–1813.
- Hess, B., H. Bekker, ..., J. G. E. M. Fraaije. 1997. LINCS: a linear constraint solver for molecular simulations. *J. Comput. Biol.* 18:1463–1472.
- Bussi, G., D. Donadio, and M. Parrinello. 2007. Canonical sampling through velocity rescaling. *J. Chem. Phys.* 126:014101.
- Berendsen, H. J. C., J. P. M. Postma, ..., J. R. Haak. 1984. Molecular dynamics with coupling to an external bath. *J. Chem. Phys.* 81:3684–3690.

Supporting Material for

Conformational states of melittin at a bilayer interface

Magnus Andersson,^{*}† Jakob P. Ulmschneider,[†] Martin B. Ulmschneider,[‡] and Stephen H. White^{*}

^{*} Department of Physiology and Biophysics, University of California, Irvine, USA; [†]Institute of Natural Sciences, Shanghai Jiao Tong University, 800 Dongchuan Road, Shanghai, 200240 Shanghai, China; [‡]Department of Crystallography, Institute of Structural and Molecular Biology, Birkbeck College, University of London, Malet Street, London WC1E 7HX, U.K.;

[†]Present address: Science for Life Laboratory, Department of Biochemistry and Biophysics, Stockholm University, SE-106 91 Stockholm, Sweden

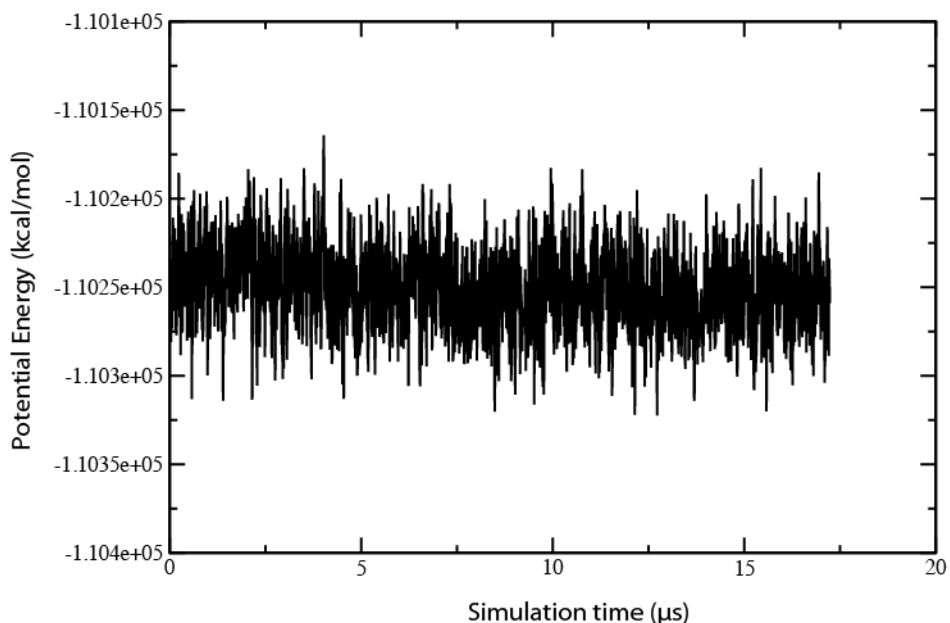


Figure S1. Energetic stability of the CHARMM simulation system in the isothermic-isobaric (NPT) ensemble. The potential energy (kcal/mol) includes the bonded and non-bonded terms for the entire system (2 melittin peptides, 264 DOPC lipids, 10,686 water molecules, and 24 Cl^- ions).

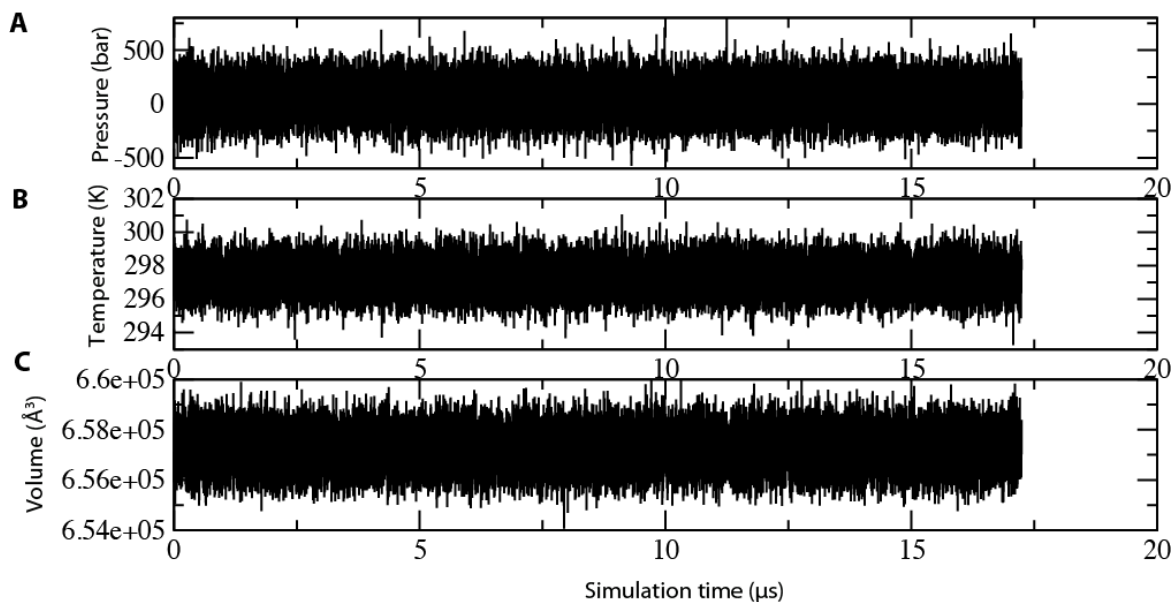


Figure S2. Stability of Berendsen baro- and thermostats, and volume variation of the simulation cell in the CHARMM simulation system. The evolution of (A) pressure (bar) and (B) temperature (K) show that the simulation system was devoid of any cold/hot spots, which can lead to problems by numerical overflow. (C) The evolution of the simulation box volume (\AA^3) further demonstrates the stability of the system.

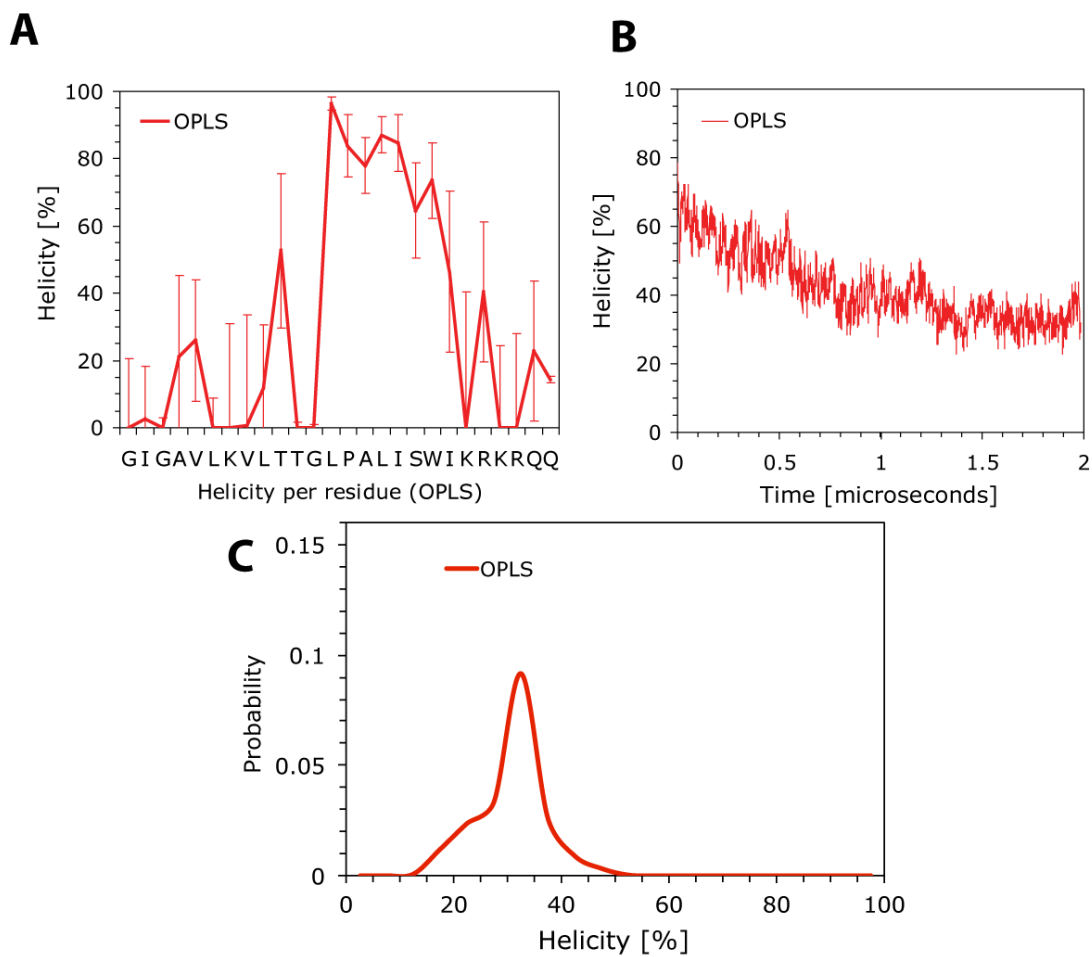
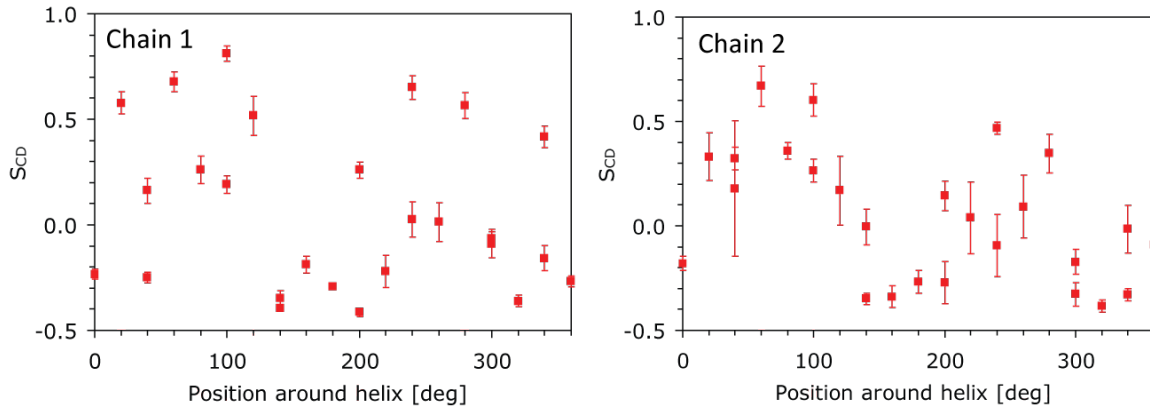


Figure S3. Helicity and conformational distribution of melittin as determined via MD simulation using the OPLS forcefield. The helicity per residue for MLT1 and MLT2 are reported in (A) and the corresponding evolution of the helicity are shown in (B). The conformational distributions over the entire 17 μ s simulation are shown in (C).



Position [deg]	residue	S _{CD} (chain 1)	S _{CD} (chain 2)
0	GLY-1	-0.234	-0.179
100	ILE-2	0.191	0.263
200	GLY-3	0.259	0.144
300	ALA-4	-0.064	-0.172
40	VAL-5	0.162	0.323
140	LEU-6	-0.394	-0.348
240	LYS-7	0.651	0.467
340	VAL-8	0.417	-0.330
80	LEU-9	0.261	0.359
180	THR-10	-0.292	-0.268
280	THR-11	0.565	0.347
20	GLY-12	0.577	0.332
120	LEU-13	0.517	0.169
220	PRO-14	-0.222	0.039
320	ALA-15	-0.361	-0.385
60	LEU-16	0.678	0.669
160	ILE-17	-0.189	-0.339
260	SER-18	0.013	0.091
360	TRP-19	-0.269	-0.089
100	ILE-20	0.811	0.602
200	LYS-21	-0.415	-0.272
300	ARG-22	-0.089	-0.328
40	LYS-23	-0.250	0.179
140	ARG-24	-0.346	-0.005
240	GLN-25	0.027	-0.094
340	GLN-26	-0.158	-0.016

Figure S4. S_{CD} order parameter $S_{CD} = \langle (1/2)(3\cos^2 q - 1) \rangle$ for the angle θ between the $C_\alpha - C_\beta$ bond and the z-axis, for each residue, averaged over the 17 μ s MD simulation using the CHARMM force field. Due to the one transition at 8 μ s, the errors (from block averaging) in chain 2 are larger than for chain 1.

Methods

The CHARMM approach

Building the system

The initial simulation system configuration was derived from the end of previous 12 ns simulation (1), which contained four melittin peptides (PDB ID 2MLT) partitioned into a 264-lipid DOPC bilayer. We removed one melittin peptide from each leaflet and solvated the system with 10,686 water molecules and added 24 Cl⁻ counterions to achieve electrical neutrality.

Molecular dynamics simulation

The μ s-timescale simulations were performed on Anton, a special-purpose computer for molecular dynamics simulations of biomolecules (2). The system was equilibrated for 10 ns using the Desmond Molecular Dynamics System, version 2.4 (D. E. Shaw Research, New York, NY, 2008) on a conventional high performance cluster before being transferred to Anton. The CHARMM22 (3) and CHARMM36 (4) force fields were used for the protein and lipids, respectively, and the TIP3P model was used for water. A reversible multiple-timestep algorithm was employed to integrate the equations of motion with a time step of 6 fs for the long-range non-bonded forces, and 2 fs for short-range non-bonded and bonded forces. All bond lengths involving hydrogen atoms were held fixed using the SHAKE algorithm. The k-space Gaussian split Ewald method (5) with a 32 x 32 x 32 grid was used to calculate long-range electrostatic interactions. A cutoff of 14 Å was used for the Lennard-Jones and short-range electrostatic interactions. The simulations were performed at constant temperature (300 K) and pressure (1 atm), using a Berendsen thermostat and semi-isotropic Berendsen barostat. Analyses and visualization were performed with VMD 1.9 (6).

The OPLS approach

One melittin peptide was embedded into the water phase of a box containing a preformed DOPC lipid bilayers made up of 72 lipids. The initial conformation was an ideal α -helix, placed 10 Å from the bilayer surface. The simulation was performed and analyzed using Gromacs version 4.0 (www.gromacs.org) (7) and hippo beta (www.biowerkzeug.com), using OPLS-AA for the protein (8), TIP3P for water (9), and united atom lipid parameters for DOPC (10). Electrostatic interactions were computed using Ewald-based PME, and a cutoff of 10 Å was used for van der Waals interactions. Bonds involving hydrogen atoms were restrained using LINCS (11). Simulations were run with a 2 fs integration time-step and neighbor lists were updated every 5 steps. All simulations are performed in the NPT ensemble, with no additional applied surface tension. Water, lipids, and the protein were each coupled separately to a v-rescale thermostat, which is a Berendsen thermostat with occasional randomizing of the velocities, with time constant $\tau_T = 0.1$ ps using weak temperature coupling (12). Atmospheric pressure of 1 bar was maintained using weak

semi-isotropic Berendsen pressure coupling with compressibility $\kappa_z = \kappa_{xy} = 4.6 \cdot 10^{-5} \text{ bar}^{-1}$ and time constant $\tau_p = 1 \text{ ps}$ (13). 2.0 μs of MD was run at 300 K.

Supporting References

1. Benz, R. W., H. Nanda, *et al.* 2006. Diffraction-based density restraints for membrane and membrane/protein molecular dynamics simulations. *Biophys. J.* 91:3617-3629.
2. Shaw, D. E., M. M. Deneroff, *et al.* 2007. Anton, a special-purpose machine for molecular dynamics simulation. *Proc. 34th Annu. Internat. Sym. Computer Architect.*
3. MacKerell, A. D., Jr., M. Feig, and C. L. Brooks, II. 2004. Extending the treatment of backbone energetics in protein force fields: Limitations of gas-phase quantum mechanics in reproducing conformational distributions in molecular dynamics simulations. *J. Comput. Chem.* 25:1400-1415.
4. Klauda, J. B., R. M. Venable, *et al.* 2010. Update of the CHARMM all-atom additive force field for lipids: validation on six lipid types. *J. Phys. Chem. B* 114:7830-7843.
5. Shan, Y., J. L. Klepeis, *et al.* 2005. Gaussian split Ewald: a fast Ewald mesh method for molecular simulation. *J. Chem. Phys.* 122:054101-054101 to 054101-054113.
6. Humphrey, W., W. Dalke, and K. Schulten. 1996. VMD: Visual molecular dynamics. *J. Mol. Graph.* 14:33-38.
7. Berendsen, H. J. C., D. van der Spoel, and R. van Drunen. 1995. GROMACS: A new message-passing parallel molecular dynamics implementation. *Comput. Phys. Commun.* 91:43-56.
8. Jorgensen, W. L., D. S. Maxwell, and J. Tirado-Rives. 1996. Development and testing of the OPLS all-atom force field on conformational energetics and properties of organic liquids. *J. Am. Chem. Soc.* 118:11225-11236.
9. Jorgensen, W. L., J. Chandrasekhar, *et al.* 1983. Comparison of simple potential functions for simulating liquid water. *J. Chem. Phys.* 79:926-935.
10. Ulmschneider, J. P., and M. B. Ulmschneider. 2009. United atom lipid parameters for combination with the optimized potentials for liquid simulations all-atom force fields. *J. Chem. Theor. Comput.* 5:1803-1813.
11. Hess, B., H. Bekker, *et al.* 1997. LINCS: A linear constraint solver for molecular simulations. *J. Comput. Biol.* 18:1463-1472.
12. Bussi, G., D. Donadio, and M. Parrinello. 2007. Canonical sampling through velocity rescaling. *J. Chem. Phys.* 126:014101.
13. Berendsen, H. J. C., J. P. M. Postma, *et al.* 1984. Molecular-dynamics with coupling to an external bath. *J. Chem. Phys.* 81:3684-3690.